川西甲基卡地区侏倭组沉积物源分析——来自碎屑锆石 U-Pb 年龄证据

秦宇龙,李名则,熊昌利,詹涵钰,徐云峰,武文辉,李峥

稀有稀土战略资源评价与利用四川重点实验室、四川省地质调查院,成都,610081

内容提要:松潘-甘孜造山带是青藏高原东北部的重要组成单元,是华北板块、扬子板块和羌塘块体的主要汇聚地区,主要由中生代浅变质沉积地层和一系列岩浆岩组成,记录了印支期以来块体之间的收敛汇聚等构造活动。其中,雅江残余盆地发育一套厚度巨大的中生代碎屑岩和岩浆岩地层组合,是研究松潘-甘孜造山带地质构造演化的理想地区之一。本文对川西甲基卡地区侏倭组的样品进行了碎屑锆石 LA-ICP-MS U-Pb 年龄测试,碎屑锆石 U-Pb 年龄存在四个峰值,分别为 231~281Ma、424~502Ma、707~983Ma、1539~1850Ma,表明扬子克拉通西缘及松潘甘孜造山带南部至少经历了四期强烈的构造—岩浆热事件,这四期事件在三叠系沉积地层中有非常清楚的记录。231~281Ma 的锆石来自东昆仑,这一年龄段的锆石最可能来自北部晚二叠世松潘洋向北俯冲于华北板块之下所形成的东昆仑岛弧花岗岩。424~502Ma 的锆石来自北秦岭,代表了加里东期南秦岭与北秦岭和华北板块的拼合事件。722~983Ma 的锆石来自扬子板块,这一年龄段的锆石最可能来自盆地东部新元古界拉伸系上扬子克拉通盆地向北西俯冲于华北板块之下所形成的南秦岭花岗岩,形成于扬子板块晋宁期陆壳增生事件。1539~1850Ma 与华北板块基底年龄特征值正相对应,是吕梁期华北克拉通东西两大块体在中部发生碰撞,华北古陆进一步固结、扩大的时间,这其中包含了继承东西块体的太古宙物质和新生的火成岩和沉积岩,在中-晚三叠世,随着秦岭洋的关闭和碰撞造山,将大量碎屑物质经华北板块南缘东西向的疏导体系注入松潘甘孜盆地。说明松潘甘孜三叠纪复理石盆地侏倭组主要接受来自东昆仑、华北板块和秦岭造山带的物质。最年轻碎屑锆石可以限定沉积岩的最大沉积年龄,侏倭组 4 颗年轻碎屑锆石加权平均计算得出 241.8±4.5Ma(n=4),推测侏倭组沉积年龄介于 231.6~249.9Ma 之间。

关键词:碎屑锆石;U-Pb 年龄;川西甲基卡地区;侏倭组;松潘-甘孜造山带

松潘-甘孜造山带是青藏高原东北部的重要组成单元,形成于古特提斯洋闭合阶段,是华北板块、扬子板块和羌塘块体的主要汇聚地区,主要由中生代浅变质沉积地层和一系列岩浆岩组成(图 1),记录了印支期以来块体之间的收敛汇聚等构造活动(Xu Zhiqin et al., 1991; Zhang Xueting et al., 2005; Roger et al, 2011)。

雅江残余盆地发育一套厚度巨大的中生代碎屑岩和岩浆岩地层组合,是研究松潘-甘孜造山带地质构造演化的理想地区之一。近年来,许多研究者对甲基卡地区关键地质体时代进行了重新定位,如对甲基卡地区岩体中锆石进行 LA-ICP-MS U-Pb 定年,获得锆石年龄为 205~223Ma(Wang Denghong et al., 2005; Hao Xuefeng et al., 2015; Tang Guofan et al., 1984)。但对围岩地层沉积物的碎屑锆石年代学方面的研究鲜有报道。

碎屑沉积物记录了盆地演化过程和物源区的性质,而碎屑锆石是沉积物中稳定的矿物之一,记录了丰富的源区信息。碎屑锆石的年龄谱不仅对源岩属性、沉积环境以及沉积盆地构造演化等多方面的信

注:本文为四川省科技计划项目(编号 2018SZ0276),全国陆域及海区地质图件更新与共享(编号 DD20190370)中国地质调查项目(编号 DD20160074、12120113049500)资助。

收稿日期:2019-07-09;改回日期:2019-09-06;网络发表日期:2019-11-27;责任编委:任东;责任编辑:黄敏。

作者简介:秦宇龙,1976 年生,工程硕士,高级工程师,地质学专业,主要从事区域地质调查、矿产勘查研究工作。通讯地址:四川省成都市人民北路一段 25 号,610081,Email:63328712@qq.com。

引用本文:秦宇龙,李名则,熊昌利,詹涵钰,徐云峰,武文辉,李峥. 2020. 川西甲基卡地区侏倭组沉积物源分析—来自碎屑锆石 U-Pb 年龄证据. 地质学报, 94(8):2400~2409, doi: 10.19762/j.cnki.dizhixuebao.2020021.

Qin Yulong, Li Mingze, Xiong Changli, Zhan Hanyu, Xu Yunfeng, Wu Wenhui, Li Zheng. 2020. Depositional provinces and tectonic background of the Zhuwo Formation in the Jiajika region, western Sichuan Province: evidence from detrital zircon U-Pb ages. Acta Geologica Sinica, 94(8):2400~2409.

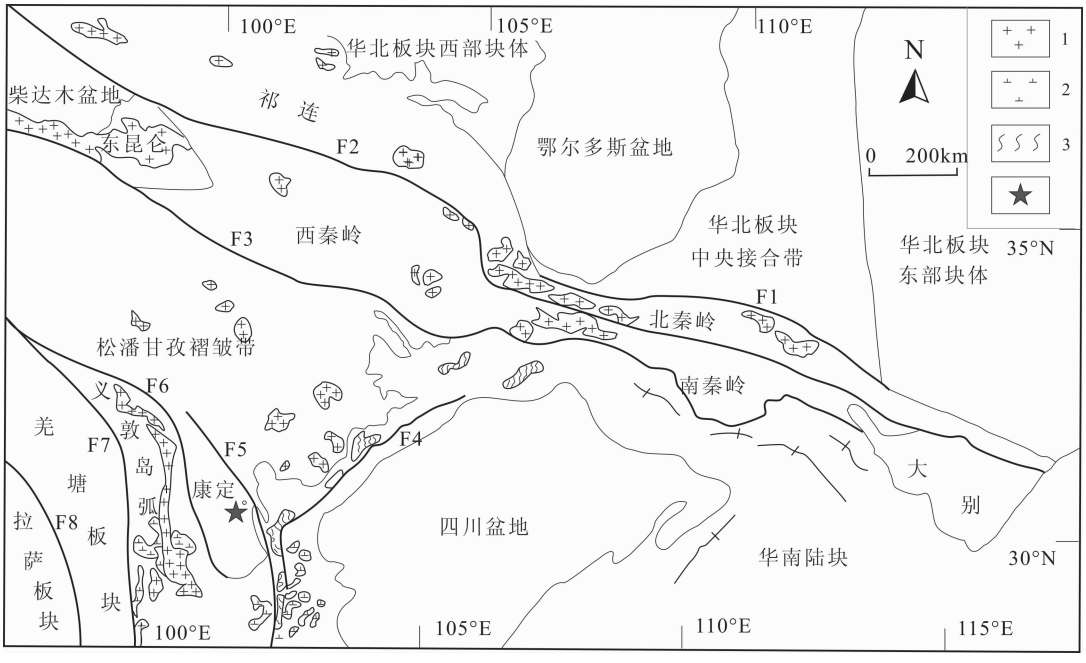

图 1　松潘甘孜-四川盆地及邻区板块构造背景及采样位置(据程裕淇, 1994 和 Enkelmann et al. ,2007,修改)

Fig. 1　Tectonic setting of Songpan-Ganze-Sichuan Basin and adjacent region with sampling sites (Modified after Cheng Yuqi,1994; Enkelmannet al. ,2007)

1—前侏罗纪侵入岩; 2—峨眉山玄武岩; 3—扬子陆块基底; 4—甲基卡采样位置; F1—柴北缘缝合带; F2—昆中缝合带; F3—阿尼玛卿缝合带; F4—龙门山构造带; F5—炉霍-道孚断裂带; F6—甘孜-理塘缝合带; F7—金沙江缝合带; F8—班公湖-怒江缝合带

1—Pre-Jurassic plutons; 2—Emeishan basalt; 3—Basement of Yangtze Block; 4—Jiajika sample localities; F1—North of Chai suture zone; F2—Kunzhong suture zone; F3—Animaqing suture zone; F4—Longmenshan tectonic belt; F5—Luhuo-Daofu fault zone; F6—Ganzi-Litang suture zone; F7—Jinshajiang suture zone; F8—Bangonghu-Nujiang suture zone

息有重要的指示意义,而且还可以限定沉积盆地最大的沉积年龄(WuYuanbao et al. ,2004;Yan Yi et al. ,2002;Cawood et al. , 2012)。雅江三叠纪复理石盆地是一个具有复杂沉积体系的多物源盆地。Nie Shangyou et al. (1994)通过将中-晚三叠世复理石地层的体积与被剥蚀掉的大别超高压变质岩上覆层的体积进行对比,推测其物源来自后者。砂岩组分或岩石地球化学分析显示盆地物源来自昆仑褶皱带(Gu Xuexiang et al. ,1994)或秦岭造山带(She Zhenbing et al. , 2006)。此外, 利用锆石 U-Pb 定年的手段在复理石地层中已发现海西期、加里东期、晋宁期、吕梁期等多年龄的碎屑锆石,但对这些锆石来源的认识仍存在分歧(Su Benxue et al. ,2006; Enkelmann et al. ,2007)和缺少必要的数据支撑。

1　地质背景

在中-晚三叠世(拉丁期-瑞替期)松潘-甘孜盆地复理石沉积期间,扬子板块西北缘沿昆仑、阿尼玛卿缝合带向北以及西南缘沿金沙江缝合带向西南的双向俯冲(许志琴等,1992),导致松潘-甘孜盆地沉积地层(西康群)在晚三叠世末期-早侏罗世发生强烈的褶皱变形并总体绿片岩化(Harrow,2005)。近乎同时, 龙门山迅速冲断隆升所产生的构造载荷使得山前形成挠曲的前渊(Meng Qingren et al. ,2005),上扬子地区海水逐渐退出,由此拉开了陆相河湖沉积的序幕。

研究区地层区划属巴颜喀拉地层区玛多-马尔康地层分区雅江小区。根据岩石地层单位划分原则,区内出露地层自下而上为:中-晚三叠世侏倭组、新都桥组和两河口组,鲜水河断裂带内有三叠纪如年各组出露。该地层小区位于鲜水河断裂带南西侧的大部分区域,在相邻的炉霍县侏倭日拉沟实测剖面上,有上三叠统菠茨沟组分布。在研究区南东部出露一套前震旦系英云闪长岩及石英闪长岩,为扬子板块结晶基底经后期混合岩化和花岗岩化的产物。

本次主要针对甲基卡地区出露的侏倭组地层开展研究,岩性以灰、深灰色碳质绢云板岩、粉砂质板岩、变质细粒长石石英砂岩、岩屑石英砂岩为主。在甲基卡马颈子附近受岩浆底辟穹窿动-热变质作用

的影响，岩性为一套含十字石红柱石二云石英片岩、含石榴石红柱石十字石片岩夹少许薄-中层状（透镜状）角岩化石英砂岩。

2 分析方法和数据处理

本次研究用于物源分析的样品 J0009N 采自川西甲基卡地区侏倭组灰色变长石石英砂岩，岩性为细粒长石石英砂岩，岩石样品呈浅灰色，岩石具细粒砂状结构，块状构造。碎屑以粒径 0.06～0.25mm 的细砂为主，0.25～0.3mm 的中砂少见，分选较好，碎屑多为棱角状-次棱角状，磨圆一般。颗粒支撑、孔隙式胶结。主要由石英、长石、云母及填隙物组成。石英：无色，棱角状-次棱角状。可见单晶石英、多晶石英和硅质岩屑，以单晶石英为主。长石：次棱角状，以聚片双晶的斜长石为主，偶见碱性长石，绢云母化严重，部分颗粒双晶模糊或不见。云母：可见黑云母和白云母，其中，黑云母棕色片状，多色性明显，；白云母无色片状，杂乱分布。填隙物：为黏土质，呈隐晶状，可见少量重结晶成细小鳞片状的绢云母。

所有样品锆石的分选在南京宏创地质勘查技术服务有限公司进行，在对样品破碎、清洗、烘干和筛选后，采用磁选和重液分离技术将锆石选出，然后在双目镜下挑选颗粒大、形态完整的锆石。测试分析在中国地质科学院地质研究所大陆构造与动力学实验室完成。锆石 U-Pb 定年工作所用的 MC-ICP-MS 为美国 Thermo Fisher 公司最新一代 Neptune Plus 型多接收等离子体质谱仪。采用的激光剥蚀系统为美国 Coherent 公司生产的 GeoLasPro 193nm。激光剥蚀以氦气作为剥蚀物质的载气，激光剥蚀束斑直径为 24～44μm，通常采用 32μm，激光能量密度为 10J/cm^2，频率为 8Hz。锆石中的 U、Pb 在 8000℃以上的高温等离子体中发生离子化，利用动态变焦扩大色散可以同时接收质量数相差很大的 U-Pb 同位素，从而进行锆石微区 U-Pb 同位素原位同时测定。每个分析点的气体背景采集时间为 4s，信号采集时间为 23s。数据分析前用国际上通用的锆石标样 91500 作为参考物质进行仪器的最佳化，使仪器达到最大的灵敏度、最小的氧化物产率（ThO+/Th+＜2%）和最低的背景值。选用 GJ-1

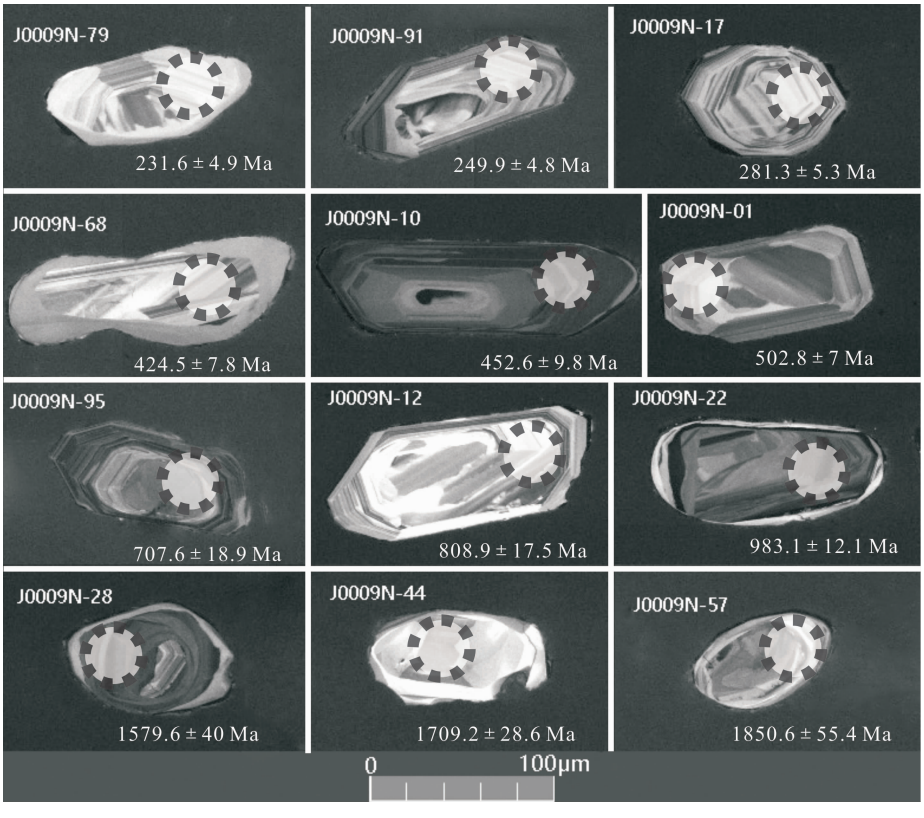

图 2 川西甲基卡地区典型锆石的背散射图像（所列为分析号和对应年龄；激光束斑直径 32μm）

Fig. 2 BSE images of typical zircons in Jiajika region, western Sichuan Province (analyzing points and corresponding ages are listed; Laser beam d=32μm)

作为辅助标样对数据的准确性进行验证。ICP-MS 数据采集选用一个质量峰采集一点的跳峰方式。每测定 5-10 个样品点,测定一组标样(一个标样 91500 点和一个 GJ-1 点)。采用中国地质大学刘勇胜博士研发的 ICPMSDataCal 程序(Liu et al.,2009)和 Ludwig 的 Isoplot 程序(Ludwig,2003)进行数据处理;年龄计算以标准锆石 91500 为外标进行同位素比值分馏。对于锆石年龄大于 1000Ma 的数据,采用$^{207}Pb/^{235}Pb$ 年龄,而对于小于 1000Ma 的数据,采用$^{206}Pb/^{238}U$ 年龄。

3　分析结果

样品 J0009N 中碎屑锆石颗粒大多呈长柱状、次圆状、次棱角状,长度从 50～150μm 不等。透射光下大部分无色透明,有些黄褐色或浅玫瑰色。对应的阴极发光图像(CL)大部分显示振荡环带,部分呈黑色、白色(图 2)。

一些锆石中可见较多的裂隙,应是由应力作用形成。部分锆石核部为早期继承性锆石。共分析测点 98 个,测试结果见表 1。其中 68 颗锆石的 Th/U 比值范围在 0.43～2.07 之间,30 颗锆石的 Th/U 比值范围在 0.02～0.38 之间。相应的$^{207}Pb/^{235}U$-$^{206}Pb/^{238}U$ 谐和关系图和年龄频率分布曲线图见图 3。参与讨论的 98 颗锆石年龄分布在 231～3758 Ma。其中 231～281Ma 共计 8 颗,424～502Ma 共计 21 颗,707～983Ma 共计 22 颗,1013～1226 Ma 共计 3 颗,1539～1850Ma 共计 27 颗,2055～2496Ma 共计 9 颗,大于 2500Ma 共计 2 颗。

4　讨论

4.1　物源区分析

综合晚三叠世侏倭组碎屑锆石 U-Pb 年龄谱总体的年龄分布特征以及锆石颗粒的内部结构特征、同位素成分特征,可以看出:在川西晚三叠世松潘-甘孜盆地中,砂岩碎屑锆石既有来自近源自形程度高的颗粒,也有可能来自经历了长距离搬运磨圆成浑圆柱、浑圆状的颗粒,其沉积物源相当复杂。

从年龄频率直方图可以看出,本文分析的样品中,有大量锆石年龄集中在 231～281Ma。Yang Jingsui et al.(2005)在晚古生代发育的东昆仑岛弧花岗岩中获得了 U-Pb 年龄为 250±20 Ma 的锆石。本文这一年龄段的锆石最可能来自北部晚二叠世松潘洋向北俯冲于华北板块之下所形成的东昆仑岛弧花岗岩。此外,样品中共有 7 颗 304～398 Ma 的锆石可能来自南秦岭(Sun Weidong et al.,2002)。

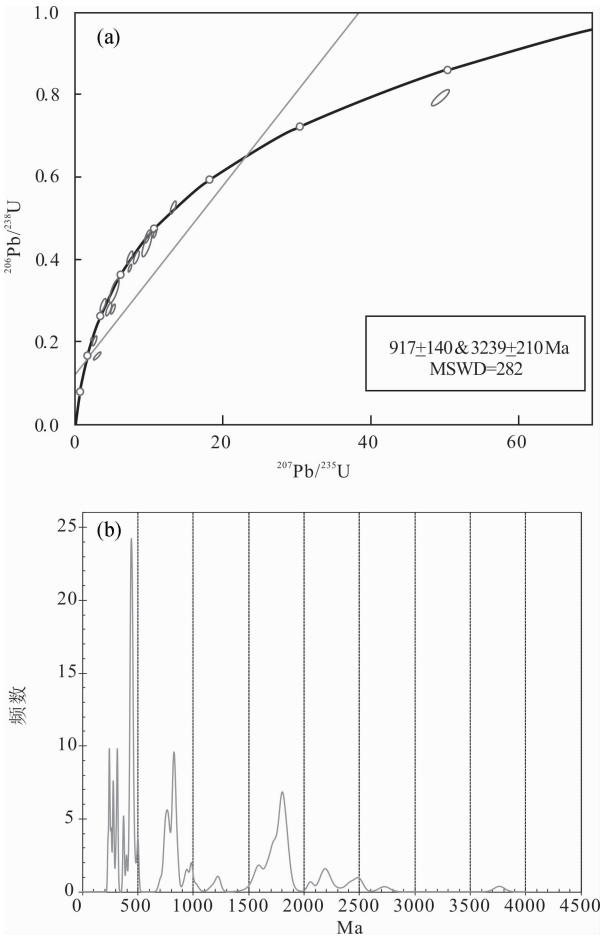

图 3　川西甲基卡地区碎屑锆石 U-Pb 谐和图(a)与频率曲线图(b)

Fig. 3　Zircon U-Pb concordia diagram (a) and relative probability plot (b) for detrital zircons in Jiajika, western Sichuan

分析中共有 21 颗 424～502Ma 的锆石年龄对应了北秦岭侵入体的形成时间,代表了加里东期南秦岭与北秦岭和华北板块的拼合事件(Ratschbachera L,2003;Hacker B R,2004),然而这一年龄的锆石在柴达木北缘高压-超高压变质带也有发现(She Zhenbing,2006)。鉴于本文所分析的锆石普遍具有较高的 Th/U 比值(表 1),多属于岩浆结晶成因,认为这一年龄的锆石更可能来自北秦岭。

共有 22 颗新元古代(707～983Ma)锆石。这在华南板块北缘、西缘以及内部都有报道,形成于扬子板块晋宁期陆壳增生事件(Zheng Yongfei et al.,2007)。分析中存在锆石年龄在 1539～1850Ma 和 2055～2496Ma 的集中,这与华北板块基底年龄特征值正相对应。2055～2496Ma 代表了华北古陆核的年龄,1539～1850 Ma 则是吕梁期华北克拉通东

表 1 川西侏倭组碎屑锆石 U-Pb 同位素分析结果表

Table 1 Analysis results of detrital zircon U-Pb isotopes

样品号及分析点号	含量(×10⁻⁶)				同位素比值						年龄(Ma)					
	Pb	Th	U	Th/U	$^{207}Pb/^{206}Pb$	1σ	$^{207}Pb/^{235}U$	1σ	$^{206}Pb/^{238}U$	1σ	$^{207}Pb/^{206}Pb$	1σ	$^{207}Pb/^{235}U$	1σ	$^{206}Pb/^{238}U$	1σ
J0009N-01	164	219.5	218.6	1.0042	0.0577	0.0006	0.6456	0.0113	0.0811	0.0012	520.4	4.6	505.7	7.2	502.8	7.0
J0009N-02	190	276.2	623.3	0.4431	0.0558	0.0005	0.5391	0.0092	0.0700	0.0011	455.6	32.4	437.8	6.2	436.4	6.7
J0009N-03	745	254.9	367.3	0.6939	0.1155	0.0008	5.0127	0.0818	0.3147	0.0050	1888.0	32.4	1821.5	15.1	1763.8	25.1
J0009N-04	90	73.7	59.4	1.2414	0.0667	0.0009	1.2604	0.0266	0.1370	0.0021	827.8	4.6	828.1	12.3	827.5	12.3
J0009N-05	835	677.1	635.9	1.0648	0.0672	0.0004	1.2554	0.0237	0.1356	0.0025	842.6	41.7	825.8	11.0	819.5	14.2
J0009N-06	64	106.7	126.7	0.8420	0.0559	0.0009	0.4908	0.0113	0.0637	0.0012	455.6	37.0	405.5	7.8	398.1	7.1
J0009N-07	419	147.5	298.3	0.4944	0.1007	0.0018	3.7556	0.2650	0.2697	0.0149	1636.1	28.6	1583.3	56.8	1539.3	75.9
J0009N-08	107	156.7	202.6	0.7736	0.0562	0.0006	0.5782	0.0129	0.0747	0.0015	457.5	27.8	463.3	8.4	464.2	9.1
J0009N-09	376	225.2	1011.5	0.2227	0.0702	0.0006	1.5013	0.0472	0.1551	0.0052	1000.0	18.5	930.9	19.4	929.6	29.0
J0009N-10	50.5	19.3	1029.2	0.0187	0.0565	0.0005	0.5672	0.0131	0.0727	0.0016	472.3	-4.6	456.2	8.6	452.6	9.8
J0009N-100	368	132.6	120.1	1.1040	0.1110	0.0008	4.9197	0.0822	0.3213	0.0051	1816.7	17.7	1805.6	15.4	1796.3	25.4
J0009N-11	87	214.1	577.4	0.3708	0.0513	0.0006	0.3162	0.0129	0.0447	0.0018	257.5	27.8	279.0	10.0	281.7	11.1
J0009N-12	192	150.9	82.2	1.8370	0.0651	0.0008	1.2001	0.0313	0.1337	0.0031	775.9	27.8	800.6	14.7	808.9	17.5
J0009N-13	344	35.4	1183.1	0.0299	0.1152	0.0010	4.4528	0.0891	0.2804	0.0062	1883.3	18.5	1722.2	17.6	1593.6	31.4
J0009N-14	804	260.8	464.6	0.5614	0.1163	0.0008	5.1925	0.0945	0.3237	0.0055	1901.9	11.6	1851.4	16.7	1807.7	27.4
J0009N-15	358	242.0	238.2	1.0158	0.0716	0.0006	1.6815	0.0525	0.1703	0.0053	975.9	41.7	1001.5	20.2	1013.6	29.2
J0009N-16	34.6	88.0	120.4	0.7311	0.0519	0.0009	0.2951	0.0068	0.0412	0.0007	279.7	37.0	262.5	5.4	260.5	4.6
J0009N-17	54.4	129.8	145.8	0.8900	0.0523	0.0008	0.3214	0.0073	0.0446	0.0008	298.2	4.6	283.0	5.7	281.3	5.3
J0009N-18	2838	753.9	363.4	2.0745	0.1569	0.0012	9.8317	0.1760	0.4542	0.0082	2433.3	12.3	2419.1	18.4	2413.8	36.9
J0009N-19	390	163.7	344.6	0.4750	0.1305	0.0093	2.9961	0.2725	0.1658	0.0058	2105.6	130.4	1406.6	69.4	989.1	32.3
J0009N-20	531	119.6	204.5	0.5848	0.1612	0.0015	10.5168	0.2040	0.4728	0.0087	2468.8	15.4	2481.4	19.9	2496.0	38.8
J0009N-21	284	243.8	173.6	1.4042	0.0646	0.0007	1.1400	0.0201	0.1279	0.0021	762.7	4.6	772.5	9.9	775.7	12.1
J0009N-22	643	410.9	598.1	0.6869	0.0726	0.0006	1.6497	0.0214	0.1648	0.0021	1011.1	16.2	989.4	8.9	983.1	12.1
J0009N-23	485	150.4	317.3	0.4741	0.1146	0.0008	5.0895	0.0635	0.3221	0.0040	1873.2	14.7	1834.4	12.3	1800.0	20.1
J0009N-24	240	187.1	150.8	1.2407	0.0654	0.0007	1.2358	0.0199	0.1370	0.0021	787.0	18.5	817.0	9.5	827.8	12.1
J0009N-25	466	85.4	850.2	0.1004	0.1289	0.0013	5.5174	0.1974	0.3101	0.0093	2083.6	18.5	1903.3	31.4	1741.0	46.0
J0009N-26	400	117.2	304.8	0.3844	0.1151	0.0008	5.1918	0.1350	0.3271	0.0081	1881.2	10.0	1851.3	23.0	1824.4	39.6
J0009N-27	120	166.0	320.8	0.5175	0.0556	0.0006	0.5400	0.0106	0.0704	0.0014	438.9	18.5	438.4	7.1	438.4	8.4
J0009N-28	799	224.2	459.7	0.4877	0.1333	0.0018	5.1083	0.1972	0.2777	0.0079	2142.6	23.1	1837.5	33.4	1579.6	40.0
J0009N-29	519	157.1	455.2	0.3451	0.1149	0.0009	4.8371	0.0864	0.3051	0.0054	1879.6	17.7	1791.4	16.2	1716.7	26.9
J0009N-30	438	376.3	331.0	1.1368	0.0645	0.0006	1.1100	0.0194	0.1248	0.0021	766.7	18.5	758.2	9.7	758.1	12.3
J0009N-31	99	171.1	161.4	1.0604	0.0546	0.0009	0.4462	0.0108	0.0593	0.0010	394.5	199.1	374.6	7.7	371.3	6.3
J0009N-32	346	58.6	706.3	0.0830	0.1192	0.0027	5.2560	0.1878	0.3193	0.0055	1946.3	42.5	1861.7	31.1	1786.2	27.3
J0009N-33	383	83.2	677.3	0.1229	0.1256	0.0011	4.9097	0.2177	0.2833	0.0112	2036.7	11.6	1803.9	37.9	1608.1	56.5
J0009N-34	183	45.6	36.0	1.2658	0.1628	0.0016	9.6727	0.4304	0.4306	0.0174	2484.9	17.0	2404.1	41.8	2308.5	78.5
J0009N-35	333	481.6	554.5	0.8686	0.0558	0.0005	0.5578	0.0083	0.0725	0.0010	455.6	41.7	450.1	5.6	451.1	5.9
J0009N-36	63.3	75.5	431.2	0.1751	0.0564	0.0005	0.5617	0.0106	0.0723	0.0012	477.8	27.8	452.7	7.1	449.7	7.4
J0009N-37	175	253.9	324.0	0.7837	0.0558	0.0006	0.5658	0.0102	0.0735	0.0012	455.6	27.8	455.3	6.8	457.3	7.5
J0009N-38	78	160.7	342.0	0.4697	0.0527	0.0006	0.3646	0.0061	0.0502	0.0008	316.7	27.8	315.6	4.7	315.5	4.7
J0009N-39	198	19.9	707.0	0.0282	0.1143	0.0010	4.3817	0.1699	0.2779	0.0103	1868.8	15.4	1708.9	32.6	1580.7	52.0
J0009N-40	438	84.6	353.6	0.2392	0.1441	0.0026	7.9466	0.1848	0.4001	0.0094	2276.9	27.0	2225.0	22.3	2169.3	43.8
J0009N-41	7.19	8.4	184.0	0.0457	0.0517	0.0009	0.2750	0.0065	0.0385	0.0007	276.0	46.3	246.7	5.2	243.7	4.3
J0009N-42	176	133.3	113.2	1.1775	0.0673	0.0008	1.3244	0.0242	0.1426	0.0022	847.8	27.8	856.4	11.0	859.6	12.7
J0009N-43	157	310.6	506.0	0.6139	0.0546	0.0006	0.3644	0.0075	0.0484	0.0010	394.5	18.5	315.5	5.6	304.8	5.9
J0009N-44	438	169.8	109.4	1.5524	0.1043	0.0010	4.3669	0.0902	0.3036	0.0057	1701.9	17.7	1706.1	18.0	1709.2	28.6
J0009N-45	170	131.8	225.1	0.5856	0.0669	0.0007	1.2688	0.0218	0.1376	0.0023	835.2	23.9	831.9	10.2	831.0	13.0
J0009N-46	71	62.9	450.0	0.1397	0.0565	0.0006	0.5613	0.0205	0.0719	0.0023	472.3	4.6	452.4	13.4	447.8	13.8
J0009N-47	101	155.0	148.3	1.0452	0.0561	0.0009	0.5535	0.0125	0.0715	0.0014	457.5	37.0	447.3	8.3	445.2	8.6
J0009N-48	143	127.6	124.9	1.0211	0.0644	0.0009	1.1185	0.0236	0.1259	0.0026	755.3	27.8	762.3	11.6	764.4	14.8
J0009N-49	77	27.5	23.9	1.1486	0.1095	0.0014	4.8333	0.0893	0.3201	0.0051	1791.1	22.4	1790.7	16.7	1790.2	25.1
J0009N-50	199	72.9	95.3	0.7652	0.1069	0.0013	4.3890	0.1259	0.2978	0.0083	1746.6	20.8	1710.3	24.4	1680.2	41.5
J0009N-51	493	405.7	441.6	0.9187	0.0667	0.0007	1.2423	0.0174	0.1350	0.0018	827.8	-4.6	819.9	8.4	816.6	10.4

续表 1

样品号及分析点号	含量($\times10^{-6}$)				同位素比值						年龄(Ma)					
	Pb	Th	U	Th/U	$^{207}Pb/^{206}Pb$	1σ	$^{207}Pb/^{235}U$	1σ	$^{206}Pb/^{238}U$	1σ	$^{207}Pb/^{206}Pb$	1σ	$^{207}Pb/^{235}U$	1σ	$^{206}Pb/^{238}U$	1σ
J0009N-52	246	23.7	820.3	0.0289	0.1165	0.0011	4.7381	0.0785	0.2949	0.0047	1902.8	15.4	1774.0	15.2	1666.1	23.7
J0009N-53	261	409.1	425.9	0.9606	0.0557	0.0006	0.5442	0.0103	0.0708	0.0012	438.9	50.9	441.2	7.0	441.3	7.6
J0009N-54	131	115.3	124.6	0.9250	0.0643	0.0007	1.1506	0.0293	0.1298	0.0031	750.0	50.9	777.5	14.1	786.6	17.9
J0009N-55	164	91.1	520.0	0.1753	0.0699	0.0006	1.5216	0.0317	0.1577	0.0032	927.8	18.5	939.1	13.1	944.1	18.3
J0009N-56	100	152.6	264.4	0.5772	0.0555	0.0007	0.5360	0.0108	0.0700	0.0012	435.2	27.8	435.8	7.3	435.9	7.3
J0009N-57	284	70.8	383.2	0.1847	0.1220	0.0017	5.6045	0.2525	0.3325	0.0114	1987.0	19.3	1916.8	39.4	1850.6	55.4
J0009N-58	121	310.8	519.0	0.5987	0.0562	0.0022	0.2965	0.0108	0.0383	0.0006	461.2	92.6	263.7	8.5	242.0	3.8
J0009N-59	1064	261.3	274.2	0.9530	0.1672	0.0014	10.8586	0.2112	0.4707	0.0087	2531.5	13.9	2511.1	20.0	2486.8	38.9
J0009N-60	526	189.0	223.8	0.8445	0.1148	0.0011	5.1451	0.0972	0.3250	0.0056	1876.9	17.0	1843.6	17.2	1814.0	27.9
J0009N-61	207	329.0	257.3	1.2789	0.0555	0.0007	0.5345	0.0102	0.0699	0.0012	431.5	4.6	434.8	6.9	435.5	7.1
J0009N-62	32.3	20.1	564.7	0.0356	0.0556	0.0005	0.5258	0.0130	0.0686	0.0017	435.2	18.5	429.0	8.7	427.7	10.1
J0009N-63	293	258.1	161.6	1.5974	0.0656	0.0007	1.1837	0.0296	0.1309	0.0032	794.4	18.5	793.0	14.0	792.9	18.5
J0009N-64	582	153.5	867.3	0.1770	0.1171	0.0009	4.9565	0.0912	0.3068	0.0055	1913.3	16.2	1811.9	16.7	1725.0	27.5
J0009N-65	137	180.0	515.7	0.3490	0.0555	0.0005	0.5728	0.0239	0.0748	0.0031	435.2	18.5	459.8	15.5	464.9	18.6
J0009N-66	215	181.9	144.3	1.2602	0.0671	0.0007	1.2757	0.0272	0.1379	0.0027	838.9	50.9	834.9	12.5	832.9	15.7
J0009N-67	224	339.3	361.8	0.9378	0.0566	0.0007	0.5616	0.0127	0.0720	0.0014	476.0	4.6	452.6	8.4	448.2	8.4
J0009N-68	199	326.9	320.6	1.0195	0.0551	0.0007	0.5178	0.0119	0.0681	0.0013	416.7	50.9	423.7	8.1	424.5	7.8
J0009N-69	476	116.1	702.7	0.1652	0.1165	0.0011	5.3125	0.1075	0.3308	0.0067	1902.8	17.0	1870.9	18.4	1842.3	32.9
J0009N-70	88	161.6	701.8	0.2303	0.0527	0.0006	0.3672	0.0089	0.0506	0.0011	322.3	27.8	317.6	6.7	318.0	6.8
J0009N-71	116	119.8	415.4	0.2885	0.0580	0.0007	0.6357	0.0181	0.0795	0.0020	527.8	189.8	499.7	11.4	493.0	11.9
J0009N-72	150	75.0	132.4	0.5666	0.0908	0.0021	2.5338	0.1381	0.2019	0.0070	1442.6	39.3	1281.8	39.9	1185.5	37.4
J0009N-73	362	98.0	211.1	0.4640	0.1300	0.0013	7.2412	0.2143	0.4037	0.0099	2097.8	17.0	2141.6	27.4	2186.1	46.0
J0009N-74	61.7	44.9	954.7	0.0470	0.0554	0.0005	0.5446	0.0111	0.0713	0.0015	427.8	-4.6	441.5	7.5	444.2	8.8
J0009N-75	688	190.9	782.4	0.2440	0.1166	0.0009	5.2348	0.1405	0.3257	0.0095	1905.6	13.9	1858.3	23.7	1817.3	46.2
J0009N-76	1522	435.5	374.7	1.1621	0.1367	0.0010	7.6557	0.1726	0.4059	0.0092	2187.0	17.7	2191.4	21.6	2196.4	42.6
J0009N-77	161	124.2	213.5	0.5819	0.0662	0.0006	1.2798	0.0275	0.1401	0.0028	813.0	18.5	836.8	12.6	845.2	15.7
J0009N-78	455	142.5	334.7	0.4258	0.1151	0.0009	5.2508	0.0980	0.3309	0.0062	1880.6	10.0	1860.9	17.1	1842.7	30.5
J0009N-79	90	247.0	212.5	1.1628	0.0514	0.0008	0.2800	0.0055	0.0395	0.0008	257.5	37.0	250.6	4.4	249.9	4.8
J0009N-80	128	206.4	161.3	1.2794	0.0555	0.0007	0.5340	0.0115	0.0698	0.0013	431.5	13.9	434.4	7.7	434.8	7.9
J0009N-81	205	40.8	76.1	0.5360	0.1836	0.0016	13.3074	0.3067	0.5256	0.0117	2687.0	11.6	2701.7	23.6	2723.0	49.9
J0009N-82	750	666.1	906.9	0.7345	0.0646	0.0005	1.0918	0.0205	0.1225	0.0023	762.7	18.5	749.4	10.3	744.7	13.5
J0009N-83	231	120.5	173.0	0.6966	0.0809	0.0007	2.3376	0.0468	0.2095	0.0041	1220.4	41.7	1223.8	14.8	1226.1	22.3
J0009N-84	1633	131.3	534.5	0.2456	0.4527	0.0035	49.4168	0.8047	0.7915	0.0128	4094.1	16.1	3980.6	21.1	3758.8	47.2
J0009N-85	246	394.2	1458.1	0.2704	0.0542	0.0004	0.4444	0.0087	0.0594	0.0011	388.9	18.5	373.3	6.3	372.2	7.0
J0009N-86	246	219.4	251.2	0.8733	0.0649	0.0010	1.0888	0.0289	0.1217	0.0022	768.5	27.8	747.9	14.3	740.2	12.6
J0009N-87	1002	275.5	406.6	0.6777	0.1407	0.0018	7.2894	0.1489	0.3755	0.0056	2236.1	21.6	2147.5	19.6	2055.3	26.9
J0009N-88	56.0	130.9	250.5	0.5227	0.0518	0.0007	0.3128	0.0058	0.0438	0.0008	276.0	-125.0	276.3	4.6	276.4	4.9
J0009N-89	221	68.9	133.6	0.5158	0.1139	0.0010	5.1423	0.1094	0.3273	0.0068	1862.7	11.6	1843.1	19.1	1825.3	33.5
J0009N-90	208	314.9	385.3	0.8174	0.0557	0.0006	0.5482	0.0113	0.0714	0.0014	438.9	50.9	443.8	7.6	444.4	8.6
J0009N-91	45.4	127.2	249.3	0.5102	0.0509	0.0008	0.2565	0.0061	0.0366	0.0008	235.3	23.2	231.8	5.0	231.6	4.9
J0009N-92	694	623.6	429.9	1.4507	0.0659	0.0006	1.1453	0.0358	0.1261	0.0038	1200.0	18.5	775.0	17.2	765.3	21.6
J0009N-93	46.3	86.6	252.7	0.3429	0.0530	0.0007	0.3669	0.0072	0.0502	0.0009	331.5	50.9	317.3	5.5	315.6	5.5
J0009N-94	1236	454.6	428.7	1.0603	0.1144	0.0009	4.8814	0.0975	0.3093	0.0063	1872.2	13.9	1799.1	17.9	1737.3	31.4
J0009N-95	350	319.1	449.5	0.7100	0.0640	0.0005	1.0243	0.0299	0.1160	0.0033	742.6	18.5	716.1	15.2	707.6	18.9
J0009N-96	528	156.2	545.5	0.2864	0.1147	0.0008	5.0525	0.1129	0.3194	0.0075	1875.9	16.2	1828.2	19.9	1786.8	37.1
J0009N-97	565	455.1	272.5	1.6701	0.0681	0.0006	1.3058	0.0213	0.1390	0.0023	872.2	-4.6	848.3	9.8	839.2	13.2
J0009N-98	605	112.7	546.8	0.2061	0.1488	0.0021	8.3392	0.3000	0.4061	0.0102	2331.8	24.7	2268.6	33.5	2196.9	47.0
J0009N-99	368	73.5	636.2	0.1156	0.1181	0.0008	5.3785	0.0853	0.3303	0.0049	1927.8	10.8	1881.4	15.0	1840.0	24.5

西两大块体在中部发生碰撞,华北古陆进一步固结、扩大的时间(Zhao Guochun,2000;Kusky,2003)。这其中包含了继承的东西块体的太古宙物质和新生的火成岩和沉积岩,在中-晚三叠世,随着秦岭洋的关闭和碰撞造山,将大量碎屑物质经华北板块南缘东西向的疏导体系(Weislogel et al.,2006;

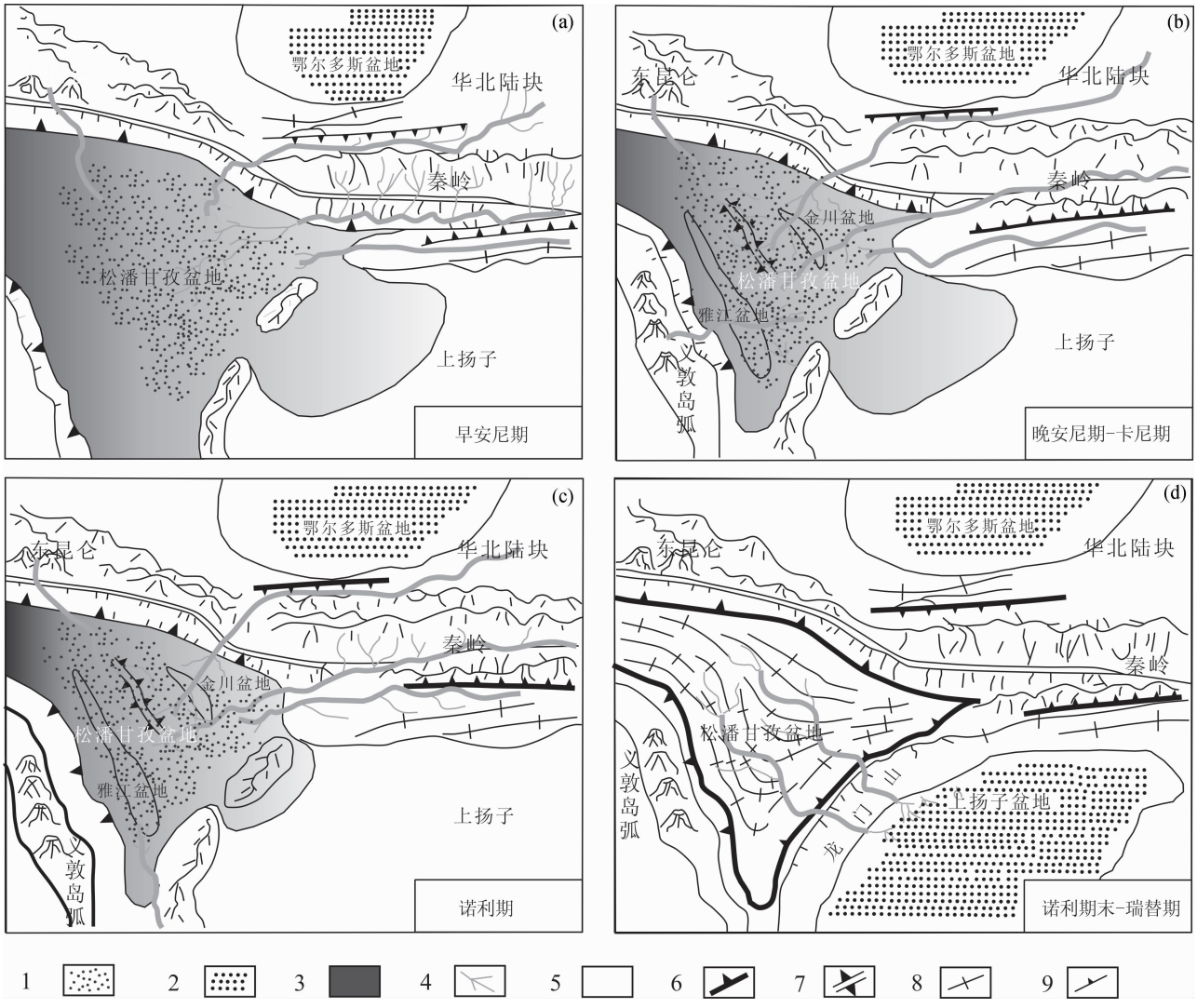

图 4 松潘甘孜-四川盆地中晚三叠世沉积体系和构造演化示意图(Deng Fei et al.,2008)

Fig. 4 Sketch map for sedimentary system and tectonic evolution of Songpan-Ganzi and Sichuan Basin in the Late Triassic(Deng Fei et al.,2008)

1—浊积岩;2—海相;3—湖湘;4—河流;5—剥蚀区;6—俯冲带;7—裂谷;8—褶皱;9—逆冲断层

1—turbidite;2—marine;3—lacustrine;4— river;5—denudation area;6—subduction zone;7—rift valley;8—fold;9—thrust fault

Enkelmann et al.,2007)注入松潘甘孜盆地。该地区卡尼期-安尼期侏倭组中的碎屑锆石出现了 231～250Ma 的峰值年龄,从锆石的 CL 图像和锆石的 Th/U 比值(表 1),可以基本确定这些锆石是典型的岩浆成因,而且较年轻锆石的形态呈柱状、次棱角状,结合岩石学研究,侏倭组中细粒砂岩属于基底式胶结,结构成熟度和分选较差。一般情况下,成分成熟度是物源区地质条件、风化程度和搬运距离远近的反映,因此可以推测侏倭组的物源来自较近的地区,应该为近源剥蚀沉积的产物。这与盆地西南部的义敦岛弧三叠纪发生的岩浆活动(229～245 Ma)(Reid et al.,2007)对应,说明义敦岛弧的碎屑物质在晚安尼期-卡尼期被输送到盆地的东部地区。诺利期地层中的碎屑锆石数据体中几乎不存在这一年龄的锆石(Su Benxun et al.,2006),说明到诺利期,义敦岛弧不再作为盆地的物源。

4.2 沉积构造环境分析

在 Weislogel et al.(2006)对松潘-甘孜复理石盆地古水系恢复的基础上,结合前人在松潘-甘孜盆地获得的碎屑锆石年龄数据(Su Benxun et al.,2006;Enkelmann et al.,2007;Deng Fei et al.,2008),本文更加全面系统地重现了松潘-甘孜盆地晚三叠世的沉积体系及其演变过程,并进一步再现了印支末期多块体汇聚拼贴作用下松潘-甘孜盆地的构造演化和古地理变迁(图 4)。

雅江三叠纪复理石盆地挟持于甘孜-理塘断裂

带与炉霍-道孚断裂带之间。在中三叠世拉丁晚期开始甘孜—理塘一带在拉伸背景下形成的裂谷,而沿炉霍-道孚断裂分布的地方也在这种拉伸背景下形成裂谷。早安尼期,携带着华北板块(中央块体)和扬子板块基底物质的河流,一进入盆地便能量消耗殆尽,使得其所搬运的物质在这里完全沉积下来,而沿秦岭造山带发育的侧向河流体系进一步延伸到盆地的南部地区。晚安尼期-卡尼期,义敦岛弧的一期构造热事件使得其成为盆地东缘的重要沉积物源。这期间沿炉霍-道孚断裂带分布的地方,在拉伸背景下形成大陆裂谷。如年各组的玄武岩、放射虫硅质岩、泥灰岩,黑色板岩构成了蛇绿岩套的上部层序是裂谷环境下形成的产物。表明在中三叠世拉丁期-卡尼期,沿炉霍-道孚断裂带分布的地方曾是裂谷环境。随着盆地双向俯冲的持续或者是源区环境的变化,携带着华北板块基底物质的水道向南扩散,使得华北板块的物质进入盆地相对南部地区。随着甘孜-理塘裂谷及炉霍-道孚裂谷的进一步扩大。炉霍-道孚裂谷北东侧的金川盆地地壳开始抬升,沉积盆地中心向西迁移,在炉霍-道孚裂谷南西侧的雅江盆地海侵范围进一步扩大。测区内扎西—瓦多一带为沉积盆地的中心,沉积了侏倭组这套深海泥质岩建造,其沉积环境为次深海—深海。其中所夹砂岩段为深海浊积扇沉积的产物。而在整个复理石沉积阶段,义敦岛弧向盆地源源不断地提供大量碎屑物质。诺利期,经过短暂的沉积以后,松潘甘孜盆地迅速发生海退,地层褶皱隆起。诺利期末-瑞替期,地壳开始逐渐抬升,松潘-甘孜造山运动至此开始。

5　结论

(1)本文所分析的锆石普遍具有较高的 Th/U(68 颗锆石的 Th/U 比值范围在 0.43～2.07 之间,30 颗锆石的 Th/U 比值范围在 0.02～0.38 之间),多属于岩浆结晶成因。

(2)松潘甘孜三叠纪复理石盆地侏倭组主要接受来自东昆仑、华北板块和秦岭造山带的物质,除此之外,在其沉积过程中,还接受了来自义敦岛弧的碎屑物质。

(3)最年轻碎屑锆石可以限定沉积岩的最大沉积年龄,侏倭组 4 颗年轻碎屑锆石加权平均计算得出 241.8±4.5Ma(n=4),推测侏倭组沉积年龄介于 231.6～249.9Ma 之间。

(4)侏倭组样品碎屑锆石有四个明显的年龄峰值区间,分别为 231～281Ma、424～502Ma、707～983Ma、1539～1850Ma 之间,表明扬子克拉通西缘及松潘甘孜造山带南部至少经历了四期强烈的构造—岩浆热事件,这四期事件在三叠系沉积地层中有非常清楚的记录。

致谢:研究过程中得到了王登红研究员、梁斌教授、郝雪峰高级工程师、何文劲高级工程师、巴金工程师等同事和朋友的帮助,在此一并致谢!

References

Andersen T. 2005. Detrital zircons as tracers of sedimentary provenance: Limiting conditions from statistics and numerical simulation. Chemical Geology, 216(3-4): 249～270.

Avigad D, Kolodner K, McWilliams M, Persing H and Weissbrod T. 2003. Origin of northern Gondwana Cambrian sandstone revealed by detrital zircon SHRIMP dating. Geology, 3(3): 227～230.

Cawood P A, Nemchin A A, Strachan R, Prave T and Krabbendam M. 2007. Sedimentary basin and detrital zircon record along East Laurentia and Baltica during assembly and breakup of Rodinia. Journal of the Geological Society, 164(2): 257～275.

Cawood P A, Hawkesworth C J, Dhuime B. 2012. Detrital zircon record and tectonic setting. Geology, 40(10): 875～878.

De Haas G J L M, Andersen T, Vestin J. 1999. Detrital zircon geochronology: New evidence for an old model for accretion of the Southwest Baltic Shield. The Journal of Geology, 107(5): 569～586.

Deng Fei, Jia Dong, Luo Liang, Li Binghai, Wu Long. 2008. The Contrast between Provenances of Songpan-Garze and Western Sichuan Foreland Basin in the Late Triassic: Clues to the Tectonics and Palaeogeography. Geological Review, 54(4): 561～573. (in Chinese with English abstract)

Enkelmann E, Weislogel A, Ratschbacher L, Elizabeth E, Axel R, Joseph W. 2007. How was the Triassic Songpan-Ganzi(Garze) basin filled: A provenance study. Tectonics, 26, T C4007.

Griffin W L, Belousova E A, Shee S R, Pearson N J, O'Reilly S Y. 2004. Archean crustal evolution in the northern Yilgarn Craton: U-Pb and Hf-isotope evidence from detrital zircons. Precambrian Research, 131(3-4): 231～282.

Gu Xuexiang. 1994. Geochemical characteristics of the Triassic Tethys-turbidites in the northwestern Sichuan, China: implications for provenance and interpretation of the tectonic setting. Geochimica et Cosmochimica Acta, 58 (21): 4615～4631.

Hacker B R, Ratschbacher L, Liou J G. 2004. Subduction, collisionand exhumation in the ultrahigh-pressure Qinling-Dabie orogen. Geological Society of London, Special Publications, 226: 157～175.

Hao Xuefeng, Fu Xiaofang, Liang Bin, Yuan Linping, Pan Meng, Tang Yi. 2015. Formation ages of granite and X03 pegmatite vein in Jiajika, western Sichuan, and their geological significance. Mineral Deposits, 34 (6): 1199～1208. (in Chinese with English abstract)

Harrow field M J, Wilson C J L. 2005. Indosinian deformation of the Songpan-Garze Fold Belt, northeast Tibet and Plateau. Journal of Structural Geology, 27: 101～117.

Kusky T M, Li Jianghai. 2003. Paleoproterozoic tectonic evolution of the North China Craton. Journal of Asian Earth Sciences, 22: 383～397.

Lan Zhongwu, Chen Yuelong, Su Benxun, Liu Fei, Zhang Hongfei. 2006. The Origin of Sandstones from the Songpan-Ganze Basin, Sichuan, China: Evidence from SHRIMP U-Pb dating of clastic zircons. Atca Sedimentologica Sinica, 24(3): 321～332. (in Chinese with English abstract)

Meng Qingren, Wang Erchie, Hu Jianmin. 2005. Mesozoic

sedimentary evolution of the northwest Sichuan basin: Implication for continued clockwise rotation of the South China block. GSA Bulletin, 117(3/4): 396～410.

Nie Shangyou, Yin An, Rowley D B, Jin Yugan. 1994. Exhumation of the Dabie Shan (Dabie Mountains) ultra-high-pressure rocks and accumulation of the Songpan-Ganzi (Garze) flysch sequence, central China. Geology, 22: 999～1002.

Ratschbachera L, Hacker B R, Calvertc A, Webbd L E, Grimmera J C, McWilliamse M O, Irelandf T, Dong S W, Hu J M. 2003. Tectonics of the Qinling (Qinling Mountains) (Central China): tectonostratigraphy, geochronology and deformation history. Tectonophysics, 366: 1～53.

Reid A, Wilson C J L, Shun Lui, Pearson N, Belousova E. 2007. Mesozoic plutons of the Yidun Arc, SW China: U/Pb geochronology and Hf isotopic signature. Ore Geology Reviews, 31: 88～106.

Roger F, Jolivet M, Cattin R. 2011. Mesozoic-Cenozoic tectono-thermal evolution of the eastern part of the Tibetan Plateau (Song-pan-Garzê, Longmen Shan area): Insights from thermochronological data and simple thermal modelling. Geological Society, London, Special Publications, 353(1): 9～25.

She Zhenbing, Ma Changqian, Mason R, Li Jianwei, Wang Guocan, Lei Yuhong. 2006. Provenance of the Triassic Songpan-Ganzi (Garze) flysch, west China. Chemical Geology, 231: 159～175.

Su Benxun, Chen Yuelong, Liu Fei, Wang Yunqiao, Zhang Hongfei, Lan Zhongwu. 2006. Geochemical characteristics and significance of Triassic sandstones of Songpan-Ganze block. Acta Petrologica Sinica, 22(4): 961～970. (in Chinese with English abstract)

Sun Weidong, Williams I S, Li Shuguang. 2002. Carboniferous and Triassic eclogites in the west ern Dabie Mountains, east-central China: Evidence for protracted convergence of the North and South China blocks. Journal of Met amorphic Geology, 20: 873～886.

Wang Denghong, Li Jiankang, Fu Xiaofang. 2005. $^{40}Ar/^{39}Ar$ dating for the Jiajika pegmatite-type rare metal deposit in western Sichuan and its significance. Geochimica, 34(6): 541～547. (in Chinese with English abstract)

Wang Wei, Li Fanglin, Bao Zhengyu. 2007. U-Pb constraints on provenance and evolution of Middle to Late Triassic Sediment in Songpan-Garze basin. Geological Science and Technology Information, 26(6): 35～44. (in Chinese with English abstract)

Weislogel A L, Graham S A, Chang E Z, Wooden J L, Gehrels G E, Yang Hengshu. 2006. Detrital zircon provenance of the Late Triassic Songpan-Ganzi (Garze) complex: Sedimentary record of collision of the North and South China blocks. Geology, 34(2): 97～100.

Wu Yuanbao, Zheng Yongfei. 2004. Study on the mineralogy of zircon and its constraints on the interpretation of U-Pb age. Chinese Science Bulletin, 49(16): 1589～1604. (in Chinese without English abstract)

Xu Zhiqin, Hou Liwei, Wang Zongxiu. 1991. New progress in the study of the Songpan-Ganzi orogenic belt. Chinese Geology, 12: 14～15. (in Chinese without English abstract)

Yan Yi, Lin Ge, Wang Yuejun, Guo Feng. 2002. The indication of continental detrital sediment to tectonic setting. Advance in Earthscience, 17(1): 85～90. (in Chinese with English abstract)

Yang Fengqing, Wang Hongmei, Yang Hengshu, Xie Shucheng. 1996. Late Triassic Carnian continental rise environment analysis of Zhuwo formation in the Tanggor Area, Zoige, Sichuan. Acta Sedimentologica Sinica, 1(3): 56～63. (in Chinese with English abstract)

Yang Jingsui, Xu Zhiqin, Li Haibing, Shi Rendeng. 2005. The paleo-Tethyan volcanism and plate tectonic regime in the A'nyemaqenregion of East Kunlun, northern Tibet Plateau, Acta Petrologica et Mineralogica, 24(5): 369～380. (in Chinese with English abstract)

Yang Zongrang. 2002. The formation and evolution of the Songpan-Garze fore-arc basin, western Sichuan. Sedimentary Geology and Tethyan Geology, 22(3): 53～59. (in Chinese with English abstract)

Zhang Guowei, Guo Anlin, Yao Pingan. 2004. Western Qinling-Songpan continental tectonic nodein China's continental tectonics. Earth Science Frontiers, 11(3): 23～32. (in Chinese with English abstract)

Zhang Xueting, Wang Bingzhang, Yu Jian, Wang Peijian, Ding Xiqi, Gu Fengbao, Zhang Xianting. 2005. Sedimentary characteristics of the Bayan Har remnant ocean basin, northwestern China. Geological Bulletin of China 24(7): 613～620. (in Chinese with English abstract)

Zhang Zongqing, Zhang Guowei, Fu Guomin, Tang Suohan, Song Biao. 1996. Age of metamorphic strata in Qinling and its tectonic significance. Science in China: Series D, 26(3): 216～222. (in Chinese without English abstract)

Zhao Guochun, Cawood P A, Wilde S A, Sun Min, Lu Liangzhao. 2000. Met amorphism of basement rocks in the Central Zone of the North China Craton: Implicat ions for Paleoproterozoic tectonic evolution. Precambrian Research, 103(1): 55～88.

Zheng Yongfei, Zhang Shaobing, Zhao Zifu, Wu Yuanbao, Li Xianhua, Li Zhengxiang, Wu Fuyuan. 2007. Contrasting zircon Hf and O isotopes in the two episodes of Neoproterozoic granitoids in South China: Implications for growth and reworking of continental crust. Lithos, 96: 127～150.

参 考 文 献

邓飞,贾东,罗良,李海滨,李一泉,武龙. 2008. 晚三叠世松潘甘孜和川西前陆盆地的物源对比:构造演化和古地理变迁的线索. 地质论评, 54(4): 561～573.

郝雪峰,付小方,梁斌,袁蔺平,潘蒙,唐屹. 2015. 川西甲基卡花岗岩和新三号矿脉的形成时代及意义. 矿床地质, 34(6): 1199～1208.

兰中伍,陈岳龙,苏本勋,刘飞,张宏飞. 2006. 四川松潘-甘孜盆地砂岩的物质来源:来自锆石 U-Pb (SHRIMP) 年龄证据. 沉积学报, 24(3): 321～332.

苏本勋,陈岳龙,刘飞,王巧云,张宏飞,兰中伍. 2006. 松潘-甘孜地块三叠系砂岩的地球化学特征及其意义. 岩石学报, 22(4): 961～970.

王登红,李建康,付小方. 2005. 四川甲基卡伟晶岩型稀有金属矿床的成矿时代及其意义. 地球化学, 34(6): 541～547.

王伟,李方林,鲍征宇. 2007. 松潘-甘孜盆地中-晚三叠世沉积物来源及演化的锆石 U-Pb 年代学制约. 地质科技情报, 26(6): 35～44.

吴元保,郑永飞. 2004. 锆石成因矿物学研究及其对 U-Pb 年龄解释的制约. 科学通报, 49(16): 1589～1604.

许志琴,侯立伟,王宗秀. 1991. 松潘-甘孜造山带构造研究新进展. 中国地质, 12: 14～15.

许志琴,侯立玮,王宗秀,付小方,黄明华. 1992. 中国松潘-甘孜造山带的造山过程. 北京:地质出版社, 73: 170～172.

闫义,林舸,王岳军,郭锋. 2002. 盆地陆源碎屑沉积物对源区构造背景的指示意义. 地球科学进展, 17(1): 85～90.

杨逢清,王红梅,杨恒书,谢树成. 1996. 四川若尔盖唐克晚三叠世卡尼期侏倭组陆隆沉积环境分析. 沉积学报, 1(3): 56～63.

杨经绥,许志琴,李海兵,史仁灯. 2005. 东昆仑阿尼玛卿地区古特提斯火山作用和板块构造体系. 岩石矿物学杂志, 24(5): 369～380.

杨宗让. 2002. 川西松潘-甘孜弧前盆地的形成及演化. 演化沉积与特提斯地质, 22(3): 53～59.

张国伟,郭安林,姚安平. 2004. 中国大陆构造中的西秦岭-松潘大陆构造结. 地学前缘, 11(3): 23～32.

张雪亭,王秉璋,俞建,王培俭,丁西岐,古风宝,张显廷. 2005. 巴颜喀拉残留洋盆的沉积特征. 地质通报, 24(7): 613～620.

张宗清,张国伟,付国民,唐索寒,宋彪. 1996. 秦岭变质地层年龄及

其构造意义.中国科学:D辑,26(3):216～222.

Depositional provinces and tectonic background of the Zhuwo Formation in the Jiajika region, western Sichuan Province: evidence from detrital zircon U-Pb ages

QIN Yulong*, LI Mingze, XIONG Changli, ZHAN Hanyu, XU Yunfeng, WU Wenhui, LI Zheng

Evaluation and Utilization of Strategic Rare Metals and Rare Earth Resource Key Laboratory of Sichuan Province, Sichuan Geological Survey, Chengdu, 610081

* *Corresponding author*: 63328712@qq.com

Abstract

The Songpan-Ganzi orogenic belt is an important part of the northeastern Qinghai-Tibet Plateau. It is the major convergent region of the North China, the Yangtze and the Qiangtang blocks. The orogenic belt consists of Mesozoic low-grade metamorphic strata and a series of magmatic rocks, and has recorded convergent events of the three blocks since the Indosinian Period. Yajiang remnant basin within the orogenic belt, in which an extremely thick sedimentary series and widespread magmatic rocks occur, is an ideal region for research on the tectonic evolution of the Songpan-Ganzi orogenic belt. This study undertakes detrital zircon LA-ICP-MA U-Pb geochronology. The results show that the zircon U-Pb age values focus on four peaks, 231～281 Ma, 424～502 Ma, 707～983 Ma, 1539～1850 Ma, respectively, indicating that the west margin of the Yangtze craton and the Songpan-Ganzi orogenic belt have been subjected to at least four stages of intensive tectonic-magmatic events that were recorded in the Triassic strata in this area. The zircons with ages 231～281 Ma are most probably from the arc granites of the east Kunlun Mountains, formed during subduction of the Permian Songpan-Ganzi Ocean downward to the North China block. The zircons with ages 424～502 Ma were derived from the Yangtze block, representing a splicing event of the south Qinling, the north Qinling and the North China blocks. The zircons with ages 722～983 Ma are from the Yangtze block, and most probably from the granites of south Qinling formed during the subduction of the Neoproterozoic extensional upper Yangtze craton basin below the North China block. The granites are the products of crustal growth event in the Jinning period. The ages 1539～1850 Ma correspond to that of basement of the North China block, when the eastern and the western parts of the North China craton collided in the central area and the North China paleo-continent was in the process of further solidification and extension. The Archean material and newly generated igneous and sedimentary rocks were inherited, and a great many of these detrital materials were carried into the Songpan-Ganzi basin through an east-west directed transport system during the closure and collisional orogeny of the south Qinling Ocean in Middle-Late Triassic Epoch. Our results suggest that the origin of the Triassic Xinduqiao Formation in the Songpan-Ganzi flysch basin was mainly the material from the east Kunlun Mountains, the North China block and the Qinling orogenic belt. The youngest detrital zircons can limit the oldest depositional age. The weighted average age of four youngest zircons is 241.8 ± 4.5 Ma, temporally constraining the deposition event of sedimentary rocks.

Key words: detrital zircon; U-Pb age; Jiajika area; western Sichuan Province; Zhuwo Formation; Songpan-Ganze orogenic belt